Power broadening of the Na-D lines in a flame-I. Time-dependent spectral and spatial properties of a flashlamp pumped dye laser

Calcar, R.A. van; Heuts, M.J.G.; Uitert, B.K. van; Meijer, H.A.J.; Hollander, Tj.; Alkemade, C.Th.

Published in:
Journal of Quantitative Spectroscopy and Radiative Transfer

DOI:
10.1016/0022-4073(81)90036-4

J. Quant. Spectrosc. Radiat. Transfer Vol. 26, No. 6, pp. 495–502, 1981
Printed in Great Britain.

0022-4073/81/120495-08$02.00/0

POWER BROADENING OF THE Na–*D* LINES IN A FLAME—I. TIME-DEPENDENT SPECTRAL AND SPATIAL PROPERTIES OF A FLASHLAMP PUMPED DYE LASER

R. A. VAN CALCAR, M. J. G. HEUTS, B. K. VAN UITERT,
H. A. J. MEIJER, TJ. HOLLANDER, and C. TH. ALKEMADE

Fysisch Laboratorium der Rijksuniversiteit Utrecht, Princetonplein 5, 3584 CC Utrecht, The Netherlands

(*Received* 17 *March* 1981)

Abstract—Prior to power broadening experiments on the Na–*D* lines in a flame (described in Part II), we investigated the time-dependent spectral and spatial properties of a flashlamp-pumped pulsed dye laser (pulse duration about 800 ns, FWHM), with Rhodamine-6G in methanol as dye liquid and an interference filter combined with a Fabry–Pérot etalon as bandwidth-restricting elements in the cavity. An experimental set-up is described that permits measurements of time-dependent spectra with a time-resolution of 10 ns and a spectral resolution of 2.5×10^5. Results are given for different concentrations of the dye solution and for two different bandwidth settings of the laser. In general the spectral profiles at different moments during the pulse are well described by Gaussian curves. The spatial profiles at different moments during the pulse are best fitted by Lorentzian curves. At small concentrations of the dye solution, the time behaviour of the shift and the bandwidth are in (qualitative) agreement with theoretical predictions, i.e. a narrowing of the bandwidth and a shift to longer wavelengths of the line centre.

INTRODUCTION

In atomic fluorescence spectroscopy, the flashlamp-pumped dye laser has become a very powerful tool in the last ten years. The long pulse duration, together with a very high spectral irradiance, make it especially useful in Saturated Atomic Fluorescence Spectroscopy (SAFS) under quasi-stationary conditions.

In applications of flashlamp-pumped dye lasers as excitation sources of atomic species in SAFS, it is important to know the spectral and spatial properties of the laser light pulse. In particular, for our measurement on power broadening of the Na–*D* lines (Part II) in a flame, it is essential to know the instantaneous spectral behaviour of the irradiating pulsed laser. In the literature, little information is available on the time-dependent properties of dye laser pulses with narrowband lasers. However, theoretical calculations of the spectral behaviour of flash-lamp-pumped dye lasers have been presented.[1,2] Experiments have been carried out by us to measure the time-dependent spectral and spatial properties. First we describe the experimental setup and measuring procedure. We then present some representative results. More details of the experimental setup and calibration are given in Refs. 3 and 4.

EXPERIMENTAL SETUP

The experimental setup is shown in Fig. 1. It consists essentially of four parts: 1, the light source; 2, the detection system; 3, the data storage; 4, the stabilization.

Light source

The light source was a flashlamp-pumped tunable dye laser (Zeiss FL3A) with a cavity length of 45 cm and a peak power of 30 kW. Two bandwidth-restricting elements were placed inside the cavity: an interference filter and a Fabry–Pérot etalon. The mean central wavelength of the laser was tuned at 5890 Å. A small fraction of the laser output was scattered from a 92% transmission neutral density filter in order to be analyzed. The time duration of the laser pulse was about 800 ns (FWHM), as measured at the central wavelength, and the repetition frequency was 0.5 Hz in all experiments.

Detection system

In order to resolve the incident light pulse spectrally, a Fabry–Pérot interferometer (Burleigh RC 110) was used in the detection channel. One of the mirrors was mounted on three stacks of piezo-electric elements. This mirror could be adjusted and displaced by applying an electric voltage to the piezo-electric elements.

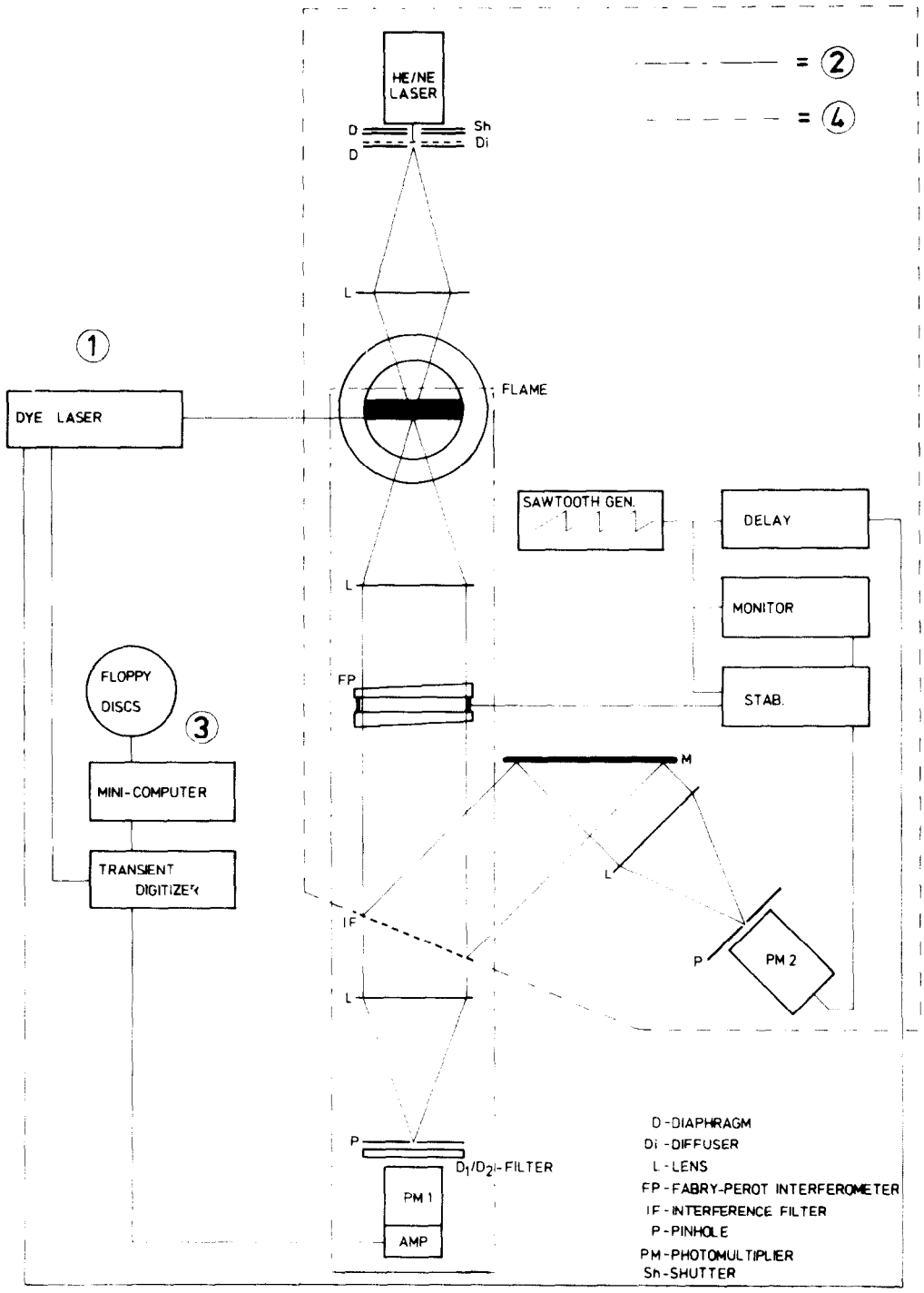

Fig. 1. Schematic diagram of the experimental arrangement. (1) light source, (2) detection system, (3) data storage, (4) stabilization system.

The overall finesse of the instrument was always 50 or more, which resulted in an instrumental profile with a transmission bandwidth of about 20 mÅ (FWHM) at a free spectral range (FSR) of 1000 mÅ. The influence of this instrumental profile on the experimental profiles was negligible due to the much larger bandwidth of the laser.

In order to resolve the incident light pulse in the detection channel temporally, a fast photomultiplier was used (EMI 9658B). With an impedance transformer and a load resistance of 1000 ohm, the rise-time of the detection system was shorter than 10 ns.

Data storage

The photomultiplier output was connected to a transient digitizer Tektronix (7912AD), being a very fast A–D converter. Light pulses were digitized with a resolution of 9 bits, both in time and intensity, and stored on a dual floppy disc memory device. The digitizing operation was monitored with a mini-computer system (Tektronix WP 2250), which could also be used for further calculations. The mini-computer was connected to a PDP 11/70 computer system for more complicated calculations (e.g., fitting theoretical curves to the experimental data).

Stabilization system

Due to changes in room temperature and to mechanical instabilities, the Fabry–PEROT interferometer would not keep its initial high finesse for more than 10–15 min. Since one series of measurements took at least two hours, a stabilization system was added (Burleigh DAS 10).

The stabilization system used an He–Ne laser as reference light source. The Ne-light was diffused and brought to focus in order to form a divergent light beam at the same spot where the dye laser was detected. After passing the Fabry–Pérot interferometer, the reference beam was deflected from the detection channel by a short wave pass interference filter (see Fig. 1) that transmitted 85% of the light from the pulsed dye laser (5890 Å) and reflected 95% of the Ne-light (6328 Å). By applying a ramp voltage to the piezoelectric elements (with a frequency of 1 Hz), the interferometer was scanned over more than two free spectral ranges. Every second scan of the interferometer was used as a test scan. During this testscan, a small additional test voltage was applied to one of the stacks in order to tilt one of the mirrors. The Ne light-peak in this test scan was then compared to that of the previous scan. Only if the finesse had increased was the test voltage maintained. In the same way, the position of the peak in the Ne-light was maintained at a fixed time interval after the start of each scan.

A shutter was placed in front of the He–Ne laser that was opened at the start of each scan, so that the Ne-light was only transmitted during the scan over the first free spectral range (see Fig. 2). This light was used by the stabilization system. Measurements of the dye laser light were carried out in the next free spectral range of the scan. In this way, the Ne-light did not interfere with the measurements.

MEASURING PROCEDURE

At the start of each new scan of the interferometer, a trigger pulse was generated by the stabilization system. After a certain chosen delay time, the dye laser was triggered and the delay time between the start time of the scan and the triggering of the dye laser was measured. As the start of each scan was fixed by the stabilization system, the delay time was a measure for the wavelength that was transmitted by the Fabry–Pérot interferometer at the moment of triggering of the dye laser (see Fig. 2). During the laser pulse, the transmitted wavelength of the interferometer shifted only by 3 μÅ, which is negligible with respect to the laser bandwidth.

After digitizing and averaging over a number of consecutive pulses (8 in most cases), the results were stored on a floppy disc memory device and labelled with the preset delay time at which the pulses were recorded. By controlling the delay time, we obtained a set of pulse registrations each labelled with a known wavelength. In each pulse registration, the instantaneous intensity was averaged over consecutive 50 ns intervals and all registrations were combined to form a set of spectra, each labelled with a time (see Fig. 3). Spectral half-intensity widths (FWHM- and central wavelengths of the spectra were then determined by fitting a Gaussian curve to the spectra with a least-squares method.

The spatial distribution of the intensity of the laser beam was measured by recording the (spectrally integrated) intensity as a function of time behind a pinhole at a large number of positions across the laser beam. The pinhole had a diameter of 0.1 mm and was placed at the position of the flame (see Fig. 1) at about 80 cm from the exit mirror of the dye laser. The half-intensity width of the spatial distribution along the principal axes of the beam cross-section was determined by fitting a Lorentzian curve to the experimental points with a least-squares method.

RESULTS

Two series of measurements were performed. In one series, a Fabry–Pérot etalon was used in the laser cavity with a spacing of 0.15 mm and a reflectance of 65%, to which we shall refer

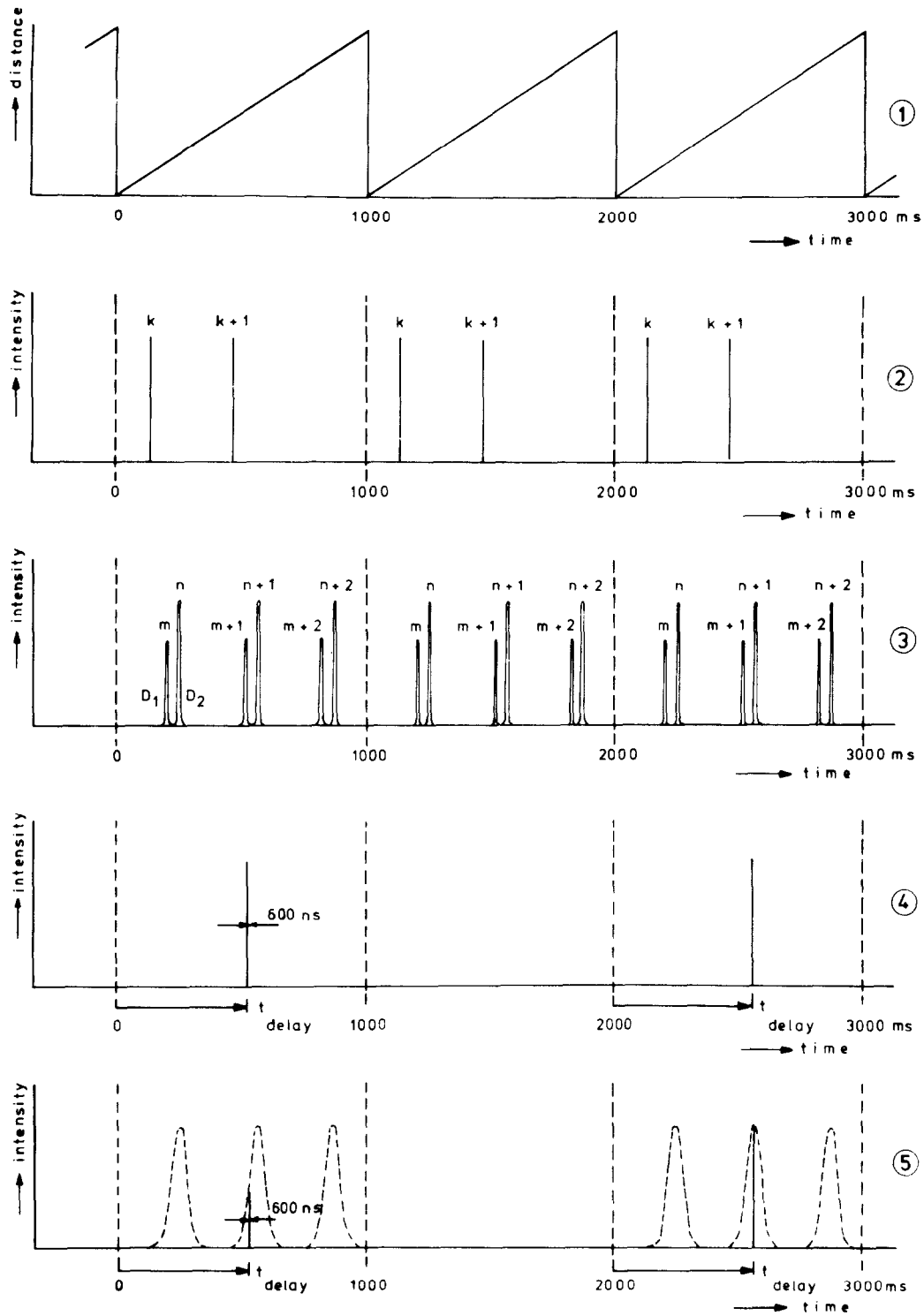

Fig. 2. Schematic overview of the measurement procedure. (1) the distance between the mirrors as a function of time. (2) the transmission bands for the Ne-light, as detected by the photomultiplier in the stabilization channel (see Fig. 1). (3) the transmission bands for the narrow Na-*D* lines of a discharge lamp, used for calibration. (4) the transmission bands for the light of the dye laser at two different delay times, as detected by the photomultiplier in the dye laser radiation. (5) the transmission bands for the fluorescence light for two different delay times, as detected by the photomultiplier in the detection channel, used for the measurements on the spectral width of the Na-*D* lines in the flame. By the use of the spectral filter behind the pinhole, only one of the Na-*D* lines was transmitted.

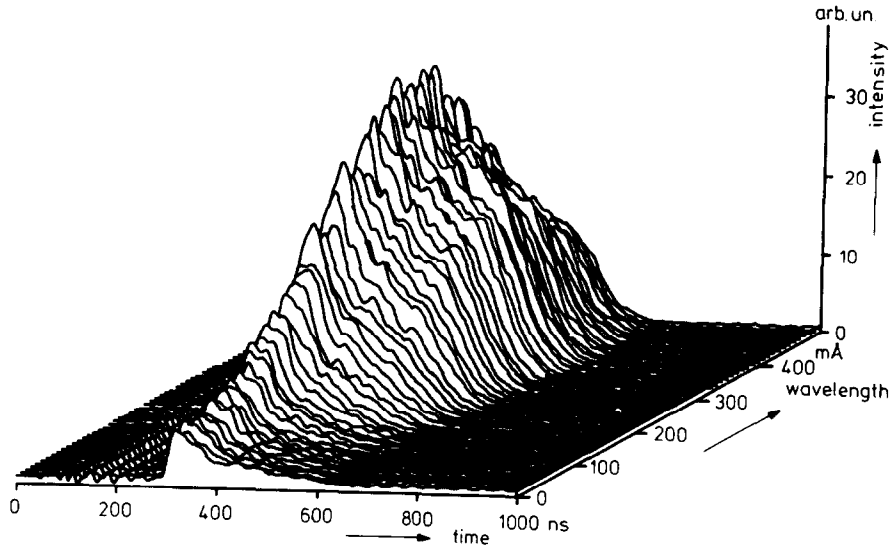

Fig. 3. Plot of the time variation of laser pulses at a large number of wavelengths. Cross-sections perpendicular to the time axis give spectra at various moments in the laser pulse.

as the narrowband etalon. In the other series, an etalon was used with a spacing of 0.10 mm and a reflectance of 33%, to which we refer as the broadband etalon.

The time-integrated output power and the duration of the pulse at the central wavelength were strongly dependent on the concentration of the dye solution in both series of measurements. This is shown in Figs. 4 and 5. The integrated output power, as well as the duration of the pulse, had a maximum at the same concentration of the dye solution: 125 ± 10 mg/l. At this concentration, the FWHM duration of the pulse for the broadband etalon was about 800 ns at the central wavelength and about 700 ns for the narrowband etalon.

Figure 6 shows typical results for the time-behaviour of the shift of the central wavelength and of the spectral half-intensity width for both etalons and at different dye concentrations. The results at large concentrations were in general less reproducible and were more structured in consecutive measurements than the results at small concentrations.

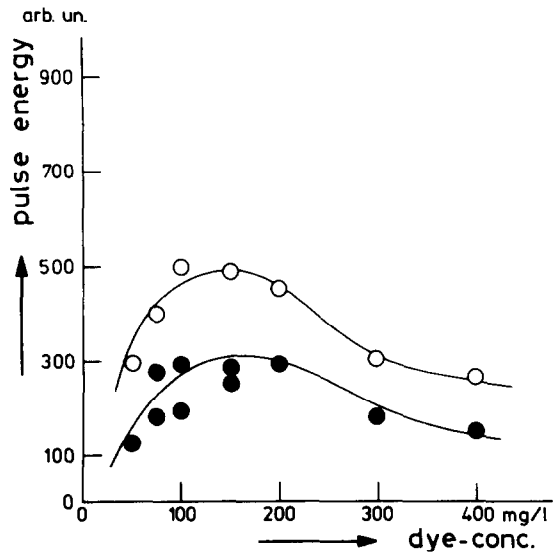

Fig. 4. Total energy in the laser pulse at different concentrations of the dye solution. (○) experimental points with the narrow band etalon in the laser cavity; (●) experimental points with the broadband etalon in the cavity. The experimental points are connected by a smoothed curve.

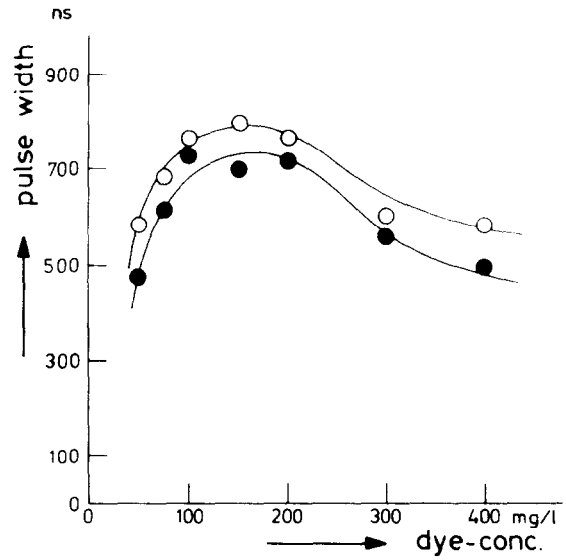

Fig. 5. The duration (FWHM) of the pulses at different concentrations of the dye solution. (●) experimental points with the narrowband etalon; (●) experimental points with the broadband etalon.

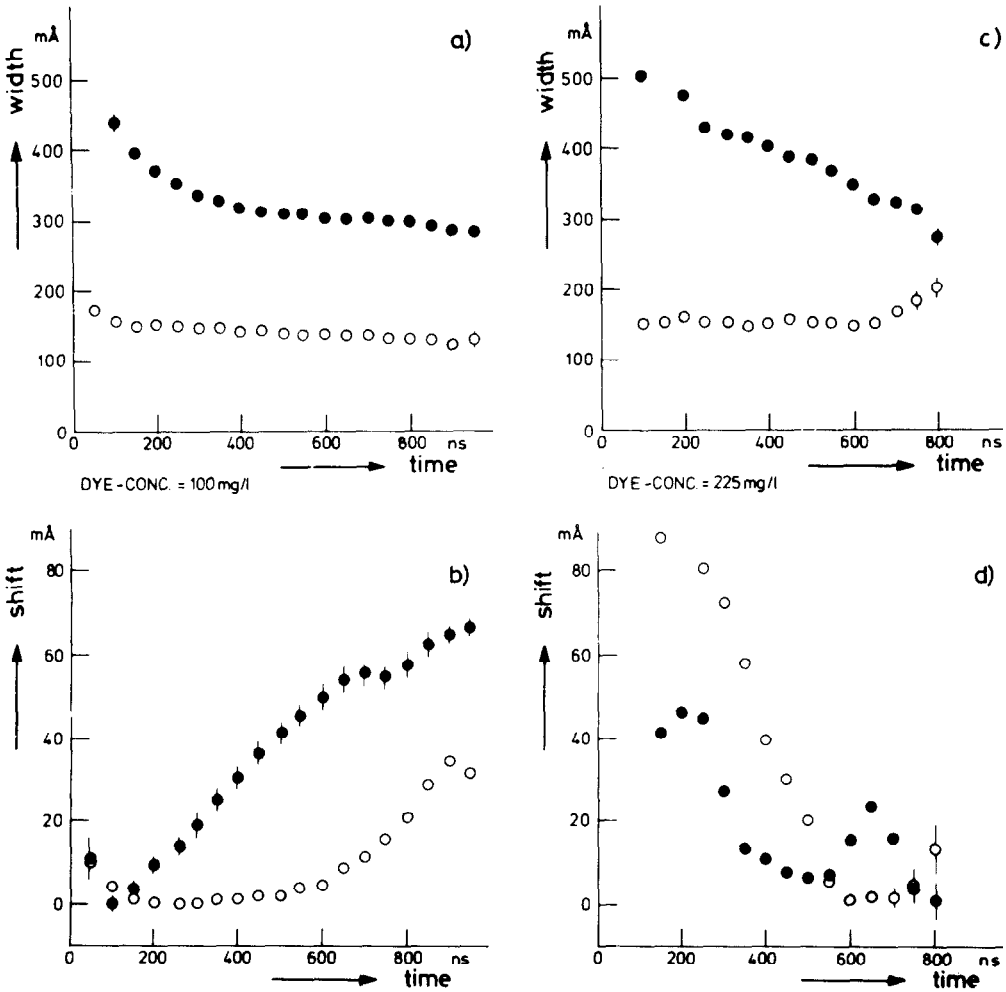

Fig. 6. Spectral width (FWHM) and shift of the central wavelength as a function of time for the narrowband (○) and broadband (●) etalon in the cavity. Figures (a) and (b) represent measurements with a small concentration of the dye solution. Figures (c) and (d) give the experimental points for a large concentration of the dye solution.

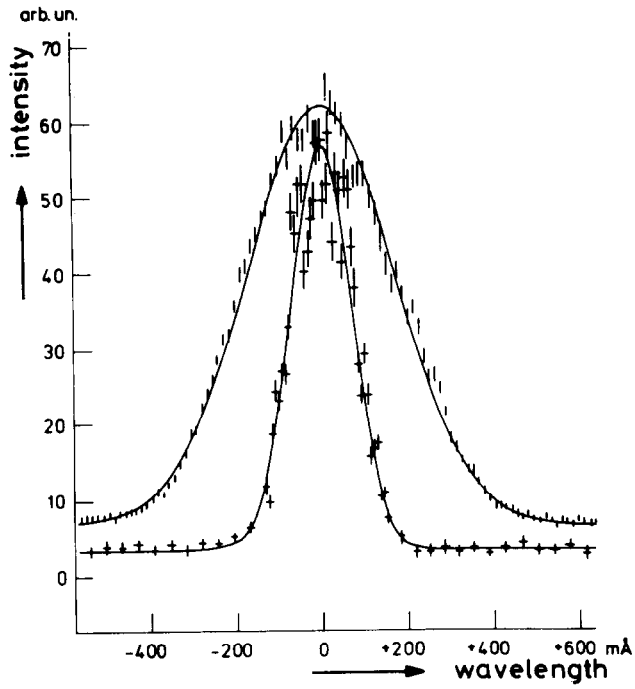

Fig. 7. A laser spectrum with the broadband respectively the narrowband etalon in the cavity. The lines represent the best fit of a Gaussian curve to the experimental points.

Figure 7 shows a typical fit of a Gaussian curve, superimposed on a constant background, to the experimental points of the spectral profile for both etalons at a small dye concentration. Within the experimental error, these fits justify the assumption of a Gaussian-shaped laser spectrum, at least near the line centre.

Numerical integration of these Gaussian spectra were compared with physical integrations of the spectra, which were obtained by measuring the laser intensity as a function of time

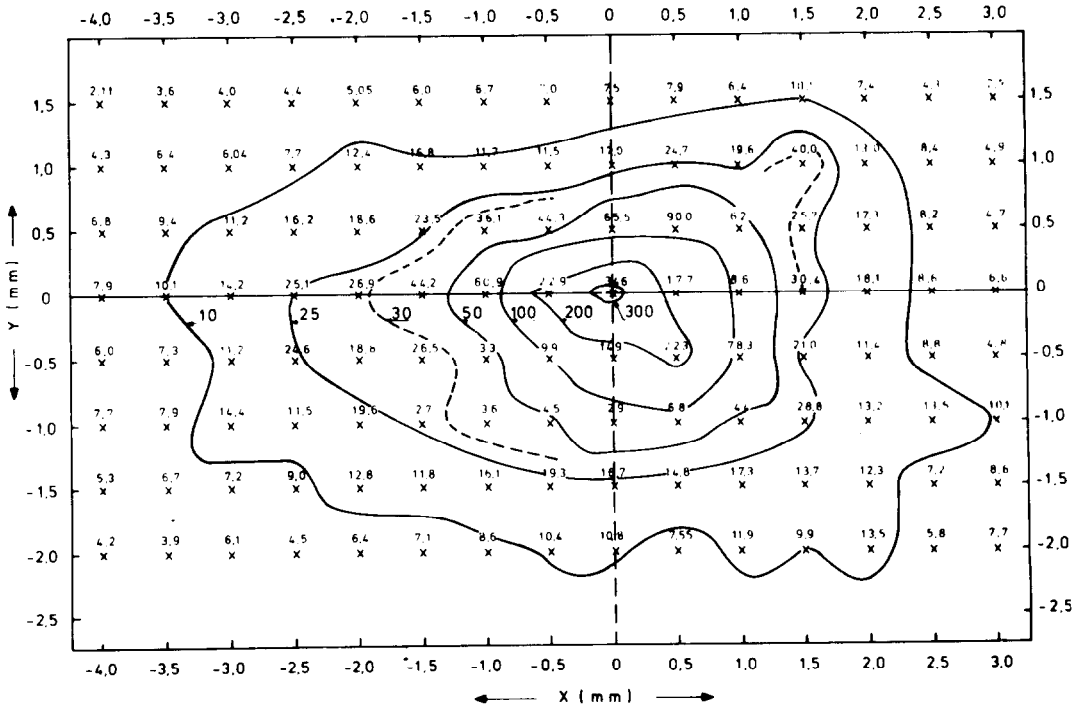

Fig. 8. Cross section of the laser beam at 300 ns after the start of the pulse. The drawn lines connect points of equal irradiance.

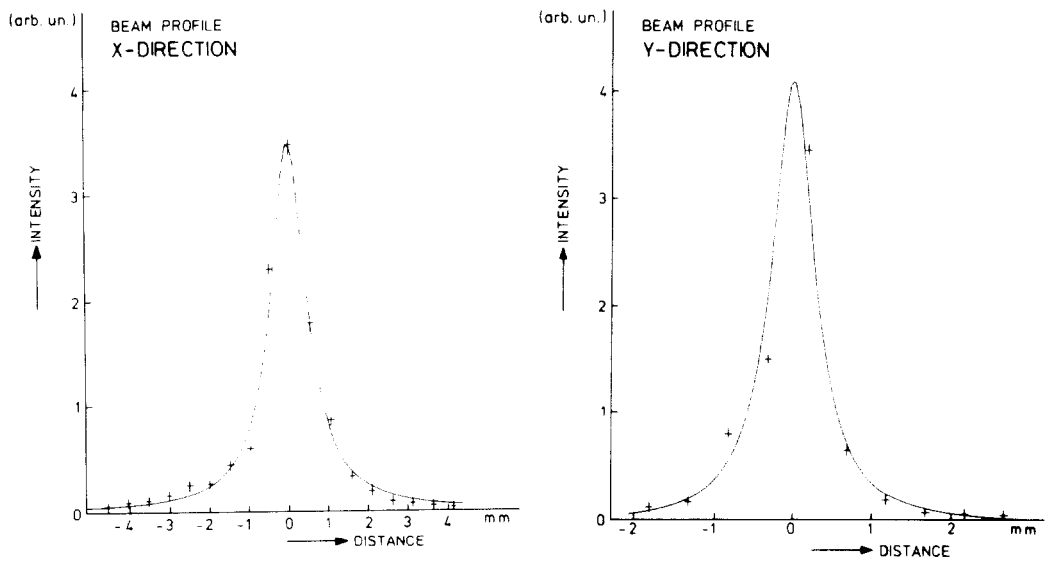

Fig. 9. The spatial distribution of the laser beam irradiance along the shaft of the pulse. The drawn lines represent best fits of a Lorentzian curve to the experimental points.

without the Fabry–Pérot interferometer in the detection channel. They appeared to be in good agreement with each other.

The spatial irradiance distribution across the beam was measured as a function of time for the broadband etalon only, because this etalon was used in the power broadening experiments (Part II). The cross section of the laser beam may be roughly described as an ellipse (see Fig. 8); distributions of the laser irradiance along the (principle) axes of the ellipse were best approximated by a Lorentz profile with a width (FWHM) of 0.28 cm for the longer axis and of 0.18 cm for the other axis. Both values were measured at 300 ns after the start of the pulse, when the spatially integrated laser pulse had its maximum value. The widths of the profiles drop gradually to the value of 0.12 cm and 0.06 cm, respectively, near the end (725 ns) of the laser pulse (see Fig. 9).

DISCUSSION

Theoretical calculations[1,2] always predict a shift of the line centre towards longer wavelengths. In our experiments, such a red shift was found at small concentrations of the dye solution. At large concentrations, however, the measurements showed a blue shift. Hence, a concentration of the dye solution can be chosen at which no shift is present in the position of the central wavelength.

A progressive narrowing of the spectrum, predicted by the theory, was indeed found, except in the measurements at large dye concentrations where this narrowing was sometimes followed by a broadening of the spectrum near the end of the pulse.

Our observations indicate that one should be very cautious when using flashlamp-pumped dye lasers as a broad-band excitation source in SAFS. It is clear that it is hazardous to draw conclusions on the behaviour of the spectral volume density of a pulsed laser beam from time-averaged measurements only.

The spatial distribution of the laser irradiance along both principal axes of the elliptic cross section was much better described by a Lorentzian profile, than by a Gaussian profile, which is often assumed to apply.

Acknowledgement—The authors wish to thank the Z. W. O. (Netherlands Organisation for Pure Scientific Research) for providing financial support for part of the instrumentation.

REFERENCES

1. J. B. Atkinson and F. P. Pace, *IEEE. J. Quantum Electron.* **QE-9**, 569 (1973).
2. P. Juramy, P. Flamant, and T. H. Meyer, *IEEE. J. Quantum Electron.* **QE-13**, 855 (1977).
3. R. A. van Calcar, *Proc. 5th Int. Conf. Spectral Line Shapes*, Berlin (1980).
4. R. A. van Calcar, Thesis, Utrecht (1980).